BMC Genomics

RESEARCH Open Access

Spatial transcriptome reveals the region-specific genes and pathways regulated by Satb2 in neocortical development

Jianfen Yang[1†], Yu Li[1†], Yiyuli Tang[1], Ling Yang[1], Chunming Guo[1] and Cheng Peng[1*]

Abstract

Background It is known that the neurodevelopmental disorder associated gene, *Satb2*, plays important roles in determining the upper layer neuron specification. However, it is not well known how this gene regulates other neocortical regions during the development. It is also lack of comprehensive delineation of its spatially regulatory pathways in neocortical development.

Results In this work, we utilized spatial transcriptomics and immuno-staining to systematically investigate the region-specific gene regulation of *Satb2* by comparing the $Satb2^{+/+}$ and $Satb2^{-/-}$ mice at embryonic stages, including the ventricle zone (VZ) or subventricle zone (SVZ), intermediate zone (IZ) and cortical plate (CP) respectively. The staining result reveals that these three regions become moderately or significantly thinner in the $Satb2^{-/-}$ mice. In the cellular level, the cell number increases in the VZ/SVZ, whereas the cell number decreases in the CP. The spatial transcriptomics data show that many important genes and relevant pathways are dysregulated in $Satb2^{-/-}$ mice in a region-specific manner. In the VZ/SVZ, the key genes involved in neural precursor cell proliferation, including the intermediate progenitor marker *Tbr2* and the lactate production related gene *Ldha*, are up-regulated in $Satb2^{-/-}$ mice. In the IZ, the key genes in regulating neuronal differentiation and migration, such as *Rnd2*, exhibit ectopic expressions in the $Satb2^{-/-}$ mice. In the CP, the lineage-specific genes, *Tbr1* and *Bcl11b*, are abnormally expressed. The neuropeptide related gene *Npy* is down-regulated in $Satb2^{-/-}$ mice. Finally, we validated the abnormal expressions of key regulators by using immunofluorescence or qPCR.

Conclusions In summary, our work provides insights on the region-specific genes and pathways which are regulated by Satb2 in neocortical development.

Keywords Satb2, Spatial transcriptomics, Neocortex, Development

[†]Jianfen Yang and Yu Li contributed equally to this work.

*Correspondence:
Cheng Peng
chengpeng@ynu.edu.cn
[1]Yunnan Key Laboratory of Cell Metabolism and Diseases, Center for Life Sciences, School of Life Sciences, Yunnan University, Kunming 650500, China

Background

Transcription factors play important roles in regulating the brain development in a series of spatiotemporally organized events [1]. The SATB2 (Special AT-rich binding protein 2) is the key one among these transcription factors, which is involved in chromatin remodeling and gene expression via binding to nuclear matrix attachment region [2]. The human genetic studies identified SATB2 as an important candidate associated with neurodevelopmental disorders [3, 4]. So it is important to investigate the molecular mechanisms of SATB2 in regulating nervous system. The works in mouse model revealed that Satb2 is expressed in many regions during embryonic development [5], and then it is highly expressed in layer 2/3 and layer 4 in cortex after birth or later stages [6]. Specifically, it is reported that Satb2 is expressed in the rhombomere region of hindbrain at embryonic day 8.5 (E8.5), and it is gradually expressed in the cortex, spinal cord and other brain regions during the embryonic development [7, 8]. Within the neocortex, the Satb2 is mainly expressed in the upper layer, but its expression is also detected in the intermediate zone (IZ) at embryonic stages [7, 9, 10]. These expression patterns imply that Satb2 may play important roles in regulating the neuron development. Previous works have revealed that Satb2 can regulate the upper-layer neuron specification [10] and callosal projection neurons [9, 11], and the Satb2 ablation leads to thinner neocortex and altered neuron migration [9, 10]. Satb2 also plays important functions in regulating the neuronal morphology [12], regionalization of retrosplenial cortex [13], development of dopaminergic neurons [14], and other developmental aspects [15]. However, previous works mainly used immuno-staining to focus on the specific and limited factors regulated by Satb2 due to the limit of traditional methods, and thus it is still necessary to comprehensively delineate the molecular pathways regulated by Satb2 in the neocortical development.

Spatial transcriptomics technologies provide the powerful tools to investigate the in situ gene expressions in the tissue in high-throughput way [16]. Recent works utilized the spatial transcriptomics to explore the brain regions for adult mouse [17], and detect spatially variable genes to mark brain sub-regions and regions [5]. The researchers also used both single cell RNA sequencing (scRNA-seq) and spatial transcriptomics to investigate the mouse cerebral cortex [18], macaque cortex [19] and human brain [20]. These works defined the neuronal subpopulations and their spatial positions, helping further understanding on the brain organization, including cell types, sub-regions, regions and marker genes. However, it is less studied on how these genes regulate the central nervous system.

Here, we utilized both spatial transcriptomics and immuno-staining to investigate the region-specific gene regulation of Satb2 in the mouse neocortical development at embryonic stages. Our work describes the morphological and cellular defects caused by *Satb2* loss in ventricle zone (VZ) or subventricle zone (SVZ), intermediate zone (IZ) and cortical plate (CP). The spatial trasncriptomics and immunofluorescence also reveal the key genes and pathways which are responsible for the abnormal development.

Methods

Preparation for mouse samples

The mice were maintained and fed in the animal facilities of Laboratory Animal Center in Yunnan University with standard conditions. The $Satb2^{+/-}$ mice were purchased from GemPharmatech Co.,Ltd in China (Strain no. T017092). The adult $Satb2^{+/-}$ were mated to generate $Satb2^{+/+}$ and $Satb2^{-/-}$ embryos and pups at embryonic day 13.5, 15.5, 17.5 and postnatal day 0. The mice were sacrificed by inhalation of excessive carbon dioxide, and another euthanasia method (neck removal) was used to ensure the death.

Immunofluorescence

The dissected fresh brains were fixed in the 4% paraformaldehyde overnight at 4 ℃, and then dehydrated by sucrose gradient (10%, 20%, 30%) for 8–12 h at 4 ℃. Then brain tissues were embedded in OCT and sections were collected at the thickness of 10 μm. The sections were fixed in methanol at -20℃ for 10 min and air dried at room temperature for 30 min, and sections were boiling in the 1X antigen repair solution (Servicebio, G1202-250ML) for 10 min. After that, sections were incubated in H_2O_2 for 20 min for bleaching non-specific HRP reaction and were further incubated in 20% goat serum (absin, abs933) 1 h for the blocking. Then primary antibodies (Supplementary Table 1) were mixed with 0.2% goat serum, and further incubation was carried out at 4 ℃ overnight. After washing, HRP-conjugated secondary antibodies (absin, abs20002) were mixed with 0.2% goat serum at room temperature for 1 h. The TSA-488 (TSA-555 or TSA-647) working solution was incubated for 10 min, and then the DAPI staining substrate (Servicebio, G1012-100ML) was incubated for 10 min. Images were captured by Olympus VS200 panoramic scanning microscope at ×20 magnification. The DAPI staining and immunofluorescences of Pax6, Tbr2 and Tbr1 were used to help the identification of VZ/SVZ, IZ and CP when measuring the region sizes and counting the cell numbers.

RNA extraction and RT-qPCR analysis

Rapidly dissected the fresh mouse neocortices at E17.5 stage. The tissues were cleaved by Trizol and RNA was extracted by chloroform. Reverse transcription was performed using PrimeScript^{TM}II 1st Stand cNDA Synthesis Kit (TaKaRa,6210 A) or HiScript II Q RT SuperMix for qPCR Kit (Vazyme, R223-01), RT-qPCR system mixing was performed using Applied Biosystems™ PowerUp™ SYBR™ Green Master Mix for RT-qPCR kit (Thermofisher, A25742) or ChamQ Universal SYBR qPCR Master Mix (Vazyme, Q711-02), and quantification was performed using QuantStudio™ 5 Real-Time PCR System. Rn18s was used as an internal reference to compare the expression difference of the same gene between different groups using the relative quantitative algorithm ΔΔCt (Supplementary Table 2).

Stereo-seq experiment

The fresh brains derived from *Satb2*$^{+/+}$ and *Satb2*$^{-/-}$ mice at E17.5 were quickly dissected, embedded in OCT, frozen on dry ice, and then stored at -80 ^{0}C. The brains were cryosectioned at the thickness of 10 μm until the target regions were reached, and the *Satb2*$^{+/+}$ coronal section and *Satb2*$^{-/-}$ coronal section were put in the same Stereo-seq chip. Then the RNA libraries were constructed by following the pipeline (version A1), in which the ssDNA staining (5 min) was imaged by using confocal (FITC, LSM800) (Supplementary Fig. 1) and the permeation time was 9 min. The cDNA was purified by using 0.8X beads. The beads were further washed twice and the obtained cDNA was used to perform PCR amplification. The PCR product was purified by 0.6X beads and the library was sequenced under MGI DNBSEQ T7 platform. The Satb2 immunofluorescence was performed to further validate the genotype of experimental samples by using the adjacent slices (Supplementary Fig. 2). One replicate was performed for the *Satb2*$^{+/+}$ and *Satb2*$^{-/-}$ mouse respectively. To validate the reliability of our spatial transcriptomics data and relevant conclusions, we utilized multiple replicates to perform immuno-staining or qPCR at population level.

Stereo-seq data processing

In the Fastq files, the read 1 contain CID (1–25 bp) and MID (26–35 bp), and the read 2 contain the cDNA sequences. We used the publicly available pipeline SAW (version 7.0) (https://github.com/STOmics/SAW) to align the raw data and generate expression matrix. Specifically, the CID sequences were mapped to the designed coordinates of the stereo-seq chip, with one base mismatch to account for sequencing and PCR errors. If the MID contained either N bases or over two bases with quality score lower than 10, the read with this MID was discarded. The CIDs and MIDs were appended to corresponding read headers, and the retained reads were aligned to the reference mouse genome (mm10) using the software STAR (version 2.7.10) [21]. The mapped reads with MAPQ > 10 were kept and counted, and then used to annotate the genes. UMIs with the same CID and gene locus were collapsed by allowing one mismatch, and these obtained data were used to generate a CID-containing expression matrix. We then used Stereopy (version 1.0.0) (https://github.com/STOmics/Stereopy) to process the expression matrix. The coordinates and overall MID counts were acquired using the st.io.read_gef function with the parameter bin_size = 50. Filter_cells function was used to exclude low-quality cells with parameters min_gene = 20 and min_n_genes_by_counts = 3. The leiden algorithm implemented in st.tl.leiden function was used to cluster spots by using the 30 principal components derived from st.tl.neighbor function, and thirteen clusters were selected by considering the brain maps from the Allen Mouse Coronal Brain Atlas (Supplementary Fig. 3). We next used FindALLMarkers function in Seurat (version 4.3.0) [22] to detect the marker genes in each cluster with parameters: $|\mathrm{Log_2FC}| > 0.25$ and $p < 0.05$.

Trajectory analysis

We used the R package monocle 2 (version 2.26.0) [23] to construct the developmental trajectory by using the spots in SVZ/VZ, IZ and CP. Integrated gene expression matrices from SVZ/VZ, IZ and CP were first exported from Seurat into Monocle to construct a CellDataSet. The significant genes (top 2,500) sorted by the q-value in differentialGeneTest function were used for cell ordering by using the setOrderingFilter function, in which the ribosome genes were excluded from the calculation. Dimensionality reduction was performed by using the reduceDimension function implemented in the DDRTree reduction method, without data normalization. The selected genes were clustered into 3 groups (C1, C2 and C3) according to the expression patterns. Gene set scores of C1, C2 and C3 were calculated by using the AddModuleScore function in Seurat.

GO enrichment pathway

The FindMarkers function in Seurat software was used to identify differentially expressed genes (DEGs) in the SVZ/VZ, IZ and CP between *Satb2*$^{+/+}$ and *Satb2*$^{-/-}$ mice by using the Wilcoxon test with the threshold P-value < 0.05 and $|\mathrm{Log_2FC}| > 0.1$. The overlapped genes between C1 gene sets and VZ/SVZ DEGs were used for pathway analysis in the VZ/SVZ. Similarly, the overlapped genes between C2 and IZ DEGs, and between C3 and CP DEGs were used for corresponding pathway analyses (Table S3). The clusterProfiler package (version 4.6.0) [24] was employed to identify enriched GO pathways associated with the selected genes, in which the

enrichGO function was utilized (ont = "ALL", qvalueCutoff=0.05, pAjustMethod = "BH"). The full pathways were listed in Table S4.

Statistics

In the statistics of immuno-staining and qPCR, the t-test was used and the data were presented as mean±SD. * $P<0.05$, ** $P<0.01$, *** $P<0.001$, **** $P<0.0001$, ns $P>0.1$.

Results

Spatiotemporal dynamics of Satb2 and other markers

The neocortical layers can be marked by proteins after birth or latter stages in mouse [6]. For example, the Pax6, Tbr2 (also called Eomes), Tbr1, Bcl11b (also called Ctip2) and Satb2 are often used to mark VZ, SVZ, layer 6/1, layer 5 and layer 2/3/4 respectively. However, it is not well known how these markers cooperatively function in the space and time during embryonic development. We then collected mouse brains at embryonic day 13.5 (E13.5), 15.5 (E15.5), 17.5 (E17.5) and postnatal day 0 (P0) to investigate the spatiotemporal relationship between Satb2 and other markers by using immunofluorescence. As shown in Fig. 1, Satb2 is laterally expressed in the neocortex near Amygdala at E13.5, and then its expression gradually spreads to many cortical regions during the development, such as the CP, retrosplenial cortex and IZ. This expression pattern is consistent with previous works [7, 9, 10, 13]. The co-staining results show that the expression relationship between Sabt2 and other markers exhibits complicated spatiotemporal dynamics during the neocortical development. At the early stage E13.5, Satb2 expression is separated from Pax6. However, some Pax6 positive cells migrate into the Satb2 positive regions, such as IZ, at E15.5 and E17.5, and then the migration of Pax6 positive cells decreases at P0. The relationship between Satb2 and Tbr2 is similar to that between Satb2 and Pax6, but with some minor differences. A small amount of Tbr2 positive and Satb2 positive cells get intermingled weakly even at E13.5. By contrast, both Tbr1 and Bcl11b are laterally co-expressed with Satb2 at E13.5. At later stages, Tbr1 and Bcl11b gradually show stronger expression in specified layers, with the trend to separate from Satb2 expression during the development. Taken together, these results show that Satb2 has complicated

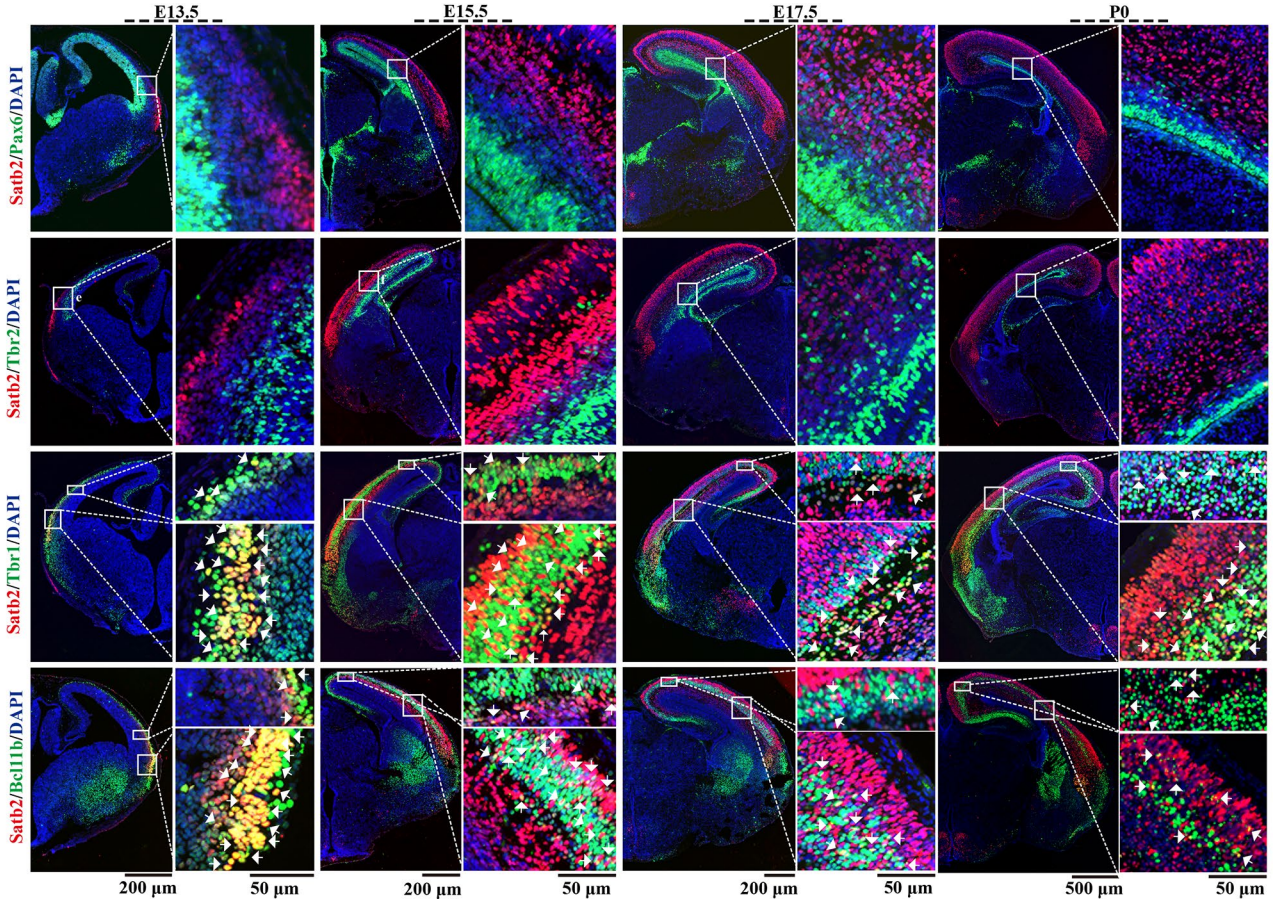

Fig. 1 The spatiotemporal relationship between Satb2 and other markers at different embryonic stages. The co-staining of Satb2 & Pax6, Satb2 & Tbr2, Satb2 & Tbr1 and Satb2 & Bcl11b are presented from the top to bottom panels, with four stages, E13.5, E15.5, E17.5 and P0. The white arrows indicate the double positive cells

spatiotemporal expression pattern with other layer markers, implying that it may has roles in regulating different neocortical regions during embryonic development.

Satb2 deficiency leads to abnormal neocortex

We then generated the *Satb2*$^{-/-}$ (*Satb2* knockout) mice to investigate the role of *Satb2* in neocortical development. In following statements, we used VZ/SVZ to denote the VZ and/or SVZ since we did not strictly distinguish these two regions in this work. The DAPI staining shows that the *Satb2*$^{-/-}$ mice exhibit abnormally thinner neocortex compared to the *Satb2*$^{+/+}$ (wild-type) mice at E17.5 (Fig. 2). Specifically, the thickness of IZ and CP significantly decreases in *Satb2*$^{-/-}$ mice in the selected brain region (Fig. 2A and B, and Supplementary Fig. 4). We also counted the cell numbers in the VZ/SVZ, IZ and CP, and the cell number varies in different regions between *Satb2*$^{+/+}$ and *Satb2*$^{-/-}$ mice (Fig. 2C). In the CP, the cell number significantly decreases in *Satb2*$^{-/-}$ mice, consistent with the decreased thickness. By contrast, there are more cells in the VZ/SVZ in *Satb2*$^{-/-}$ mice than *Satb2*$^{+/+}$ mice, though there is no significant change in thickness between these two kinds of mice. This result implies that there exists abnormally higher cell proliferation in the VZ/SVZ. We also observed weak decrease trend in total cell number in the *Satb2*$^{-/-}$ mice, but there is no significant change between the *Satb2*$^{+/+}$ and *Satb2*$^{-/-}$ mice. These results are largely consistent with previous works [9, 10] though the exact reduction degree of cortical thickness and cell number may be different due to experimental variations. Taken together, the *Satb2* loss leads to thinner IZ and CP, with cell increases in the VZ/SVZ and cell decreases in the CP.

Spatial transcriptomics capture the major neocortical regions

We then performed spatial transcriptomics experiment [25] for the *Satb2*$^{+/+}$ and *Satb2*$^{-/-}$ mice at E17.5 stage. The spatial domains derived from the spatial transcriptomics resemble the major brain regions in the Allen brain maps (Fig. 2D and E). Furthermore, we identified three sub-domains (cluster 4, 8 and 11) in the neocortex, with high similarity to the VZ/SVZ, IZ and CP derived from immuno-staining (Fig. 2F). We then used the markers to further annotate these three regions. The result shows that the cluster 11 is enriched with the expressions of *Sox2*, *Pax6* and *Tbr2*, cluster 8 is enriched with the expressions of *Rnd2* and *NeuroD1*, and the cluster 4 is enriched with the expressions of *Tbr1*, *Bcl11b* and *Sox5* (Fig. 2F and G). Taken the gene expression pattern and spatial position together, these three sub-domains in neocortex capture the major regions of VZ/SVZ, IZ and CP respectively, though minor variations may exist.

Spatial transcriptomics reveal the region-specific regulation

We next computationally inferred the pseudo-trajectory by using the spatial transcriptomics data from the VZ/SVZ, IZ and CP. As shown in Fig. 3A, the developmental trajectory mainly goes from VZ/SVZ to IZ, and then to CP in both the *Satb2*$^{+/+}$ and *Satb2*$^{-/-}$ mice, consistent with the known developmental procedure [6]. With this pseudo-trajectory, we mapped gene expressions over the pseudotime and clustered these trajectory-relevant genes according to their expression patterns (Fig. 3B). Three gene sets, named as C1, C2 and C3, were identified, in which the C1, C2 and C3 genes are mainly expressed in the VZ/SVZ, IZ and CP respectively (Fig. 3C). Hence, we identified the differentially expressed genes (DEGs) in the VZ/SVZ, IZ and CP by using the C1, C2 and C3 genes respectively, and we found that many genes are up-regulated or down-regulated in the VZ/SVZ, IZ and CP respectively (Fig. 3D, Supplementary Table 3).

We next performed pathway analyses by using the VZ/SVZ-specific, IZ-specific and CP-specific DEGs derived from C1, C2 and C3 gene sets respectively. The pathways derived from up-regulated and down-regulated DEGs were separately presented to show more details. However, since the genes can play positive or negative roles in regulating neurogenesis, both up-regulated and down-regulated gene expressions can contribute to the same pathway. As shown in Fig. 3E, the DEGs in the VZ/SVZ are enriched with canonical glycolysis, mitotic cell cycle phase transition, neural precursor cell proliferation, stem cell differentiation, chromatin remodeling, and etc. (Fig. 3E). These pathways suggest that the neural precursor cells in VZ/SVZ undergo abnormal cell division and proliferation. Specifically, the pluripotent factor *Sox9*, an important gene to induce and maintain neural stem cells [26], is up-regulated in the *Satb2*$^{-/-}$ mouse. It is reported that the lactate produced in glycolysis can regulate the progenitor cell division and proliferation in the developing mouse neocortex [27]. In our result, the canonical glycolysis is among the most enriched pathways, implying that the enhanced glycolysis caused by *Satb2* loss may contribute to the observed cell proliferation in the VZ/SVZ. Actually, we found up-regulation of many important genes in this pathway. For example, the *Ldha*, *Aldoa* and other genes involved in lactate production are up-regulated in the *Satb2*$^{-/-}$ VZ/SVZ (Fig. 3F).

In the IZ, we observed the enriched pathways on regulation of neurogenesis, cerebral cortex radially oriented cell migration, regulation of neuron differentiation and etc. (Fig. 3E), indicating that the cells undergo abnormal development and migration in the IZ. Similar to the VZ/SVZ, many important genes involved in these pathways are dysregulated in this region, such as *Sox11* [28] and *Rnd2* [29] (Fig. 3F). Specifically, one dysregulated gene

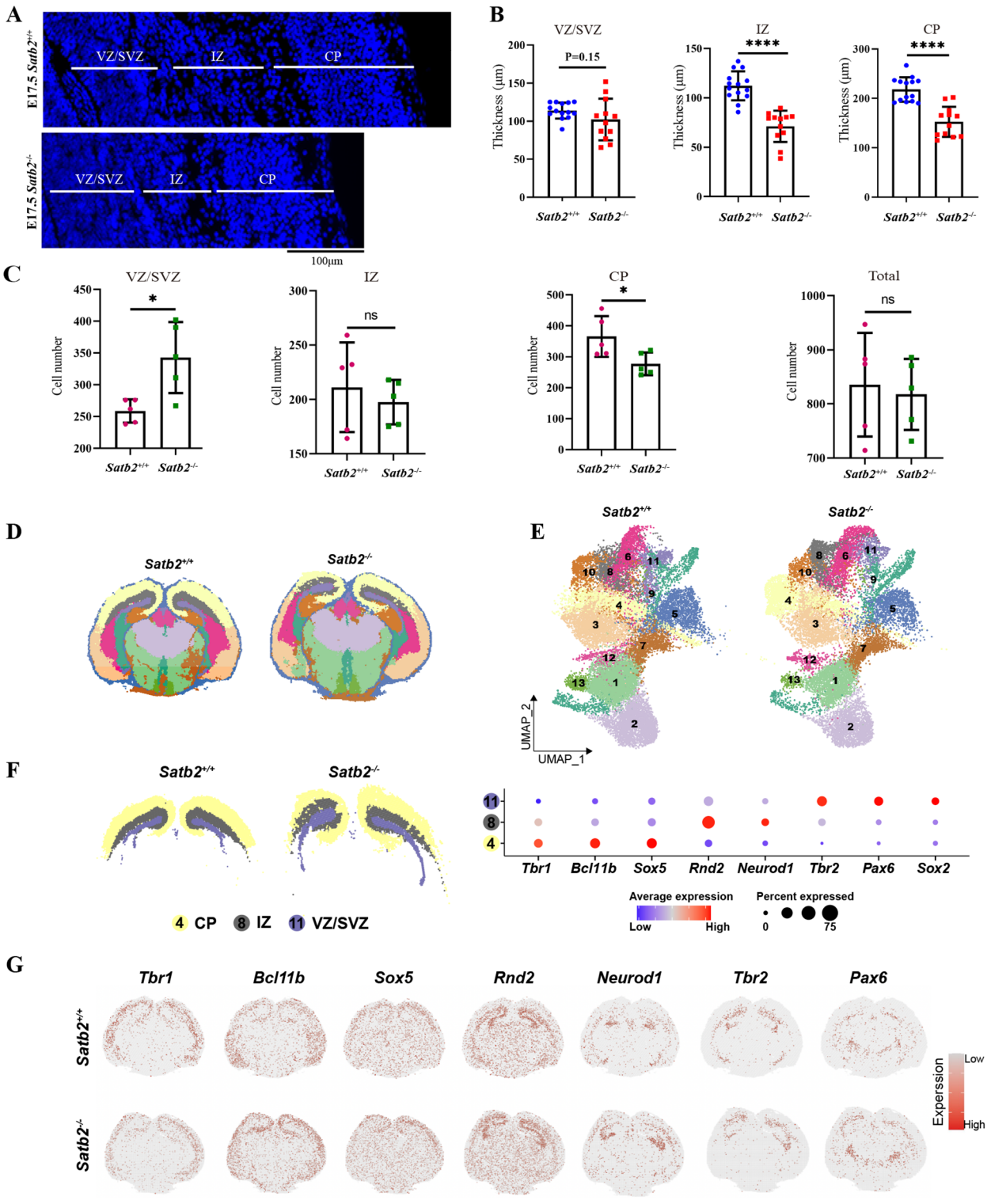

Fig. 2 The analyses of neocortical phenotype and spatial transcriptomics data. (**A**) The DAPI staining shows the abnormal neocortex in the *Satb2*-deficiency mouse. The $Satb2^{-/-}$ mouse exhibits thinner neocortex than $Satb2^{+/+}$ mouse. (**B**) The statistics on the thickness of VZ/SVZ, IZ and CP. Sample size: $Satb2^{+/+}$, 14; $Satb2^{-/-}$, 12. (**C**) The statistics on the cell number in VZ/SVZ, IZ and CP. Sample size: $Satb2^{+/+}$, 5; $Satb2^{-/-}$, 5. In (**A**), (**B**) and (**C**), the statistics were performed on the selected regions as shown in Supplementary Fig. 4. (**D**) Spatial domains derived from spatial transcriptomics data. (**E**) The UMAP visualization of spatial domain clustering. (**F**) The three spatial domains (clusters 4, 8 and 11) capture the major characteristics of VZ/SVZ, IZ and CP in both spatial positions and marker genes. The left subfigures denote the three spatial domains, and the right subfigures show the gene expression levels of layer markers. (**G**) The spatial gene expressions of marker genes

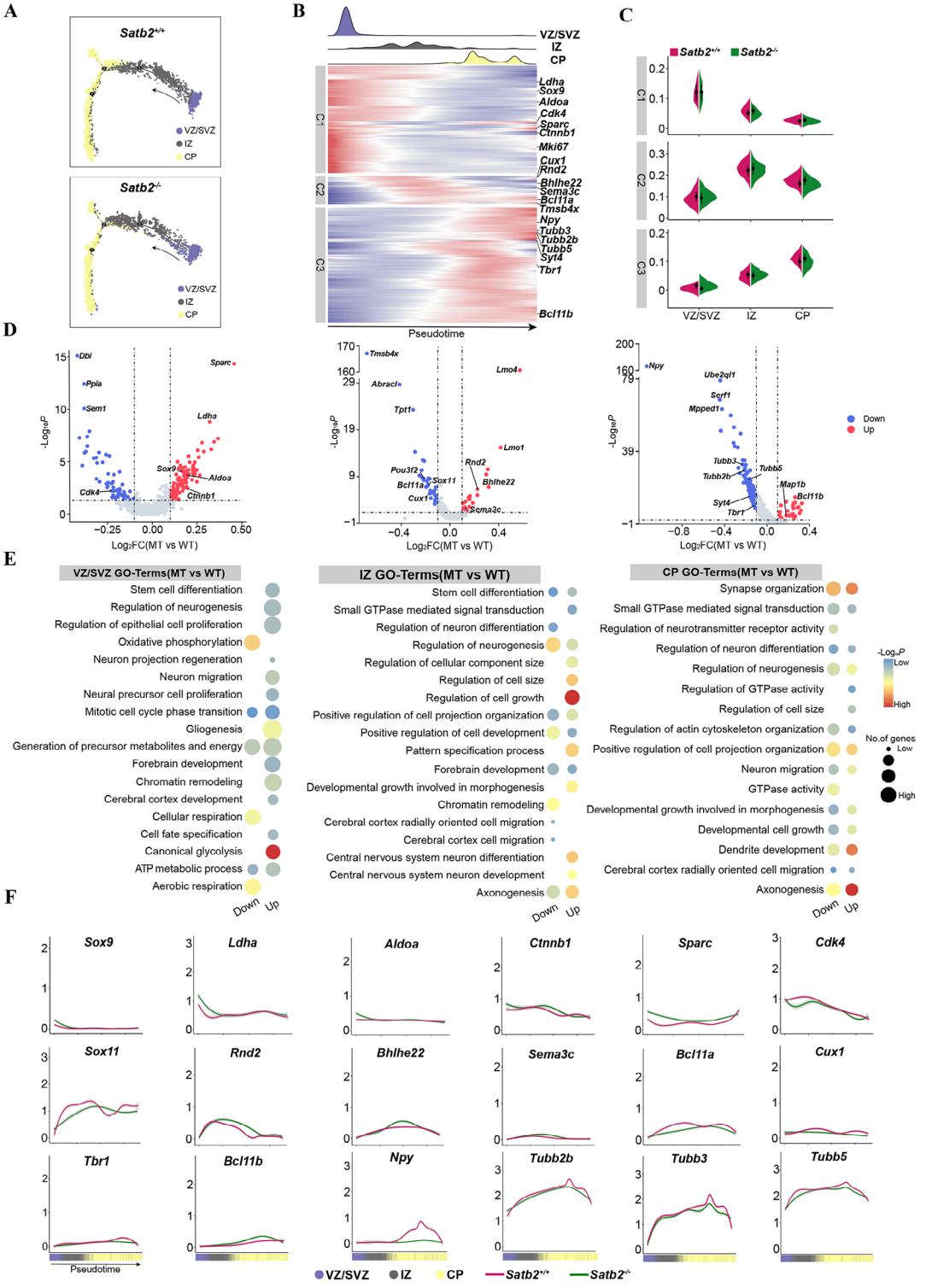

Fig. 3 The region-specific gene expressions and pathways regulated by Satb2. (**A**) The pseudo-trajectory. (**B**) The gene expression pattern along with pseudotime. The x-axis and y-axis denote the pseudo-time and representative genes respectively. The peaks in the top three panels represent the signal strength in the VZ/SVZ, IZ and CP respectively. Three gene sets, C1, C2 and C3, were identified. (**C**) The statistics on the expression levels of C1, C2 and C3 genes in the VZ/SVZ, IZ and CP. (**D**) The differentially expressed genes from the C1, C2 and C3 genes respectively. (**E**) The pathway analyses for the up-regulated and down-regulated DEGs in the VZ/SVZ, IZ and CP. Down and Up represent the pathways derived from down-regulated and up-regulated DEGs in the *Satb2*$^{-/-}$ mouse, respectively. (**F**) The expression dynamics of representative genes. In each sub-panel, the x-axis and y-axis denote the pseudotime and gene expression level respectively. MT: *Satb2*$^{-/-}$; WT: *Satb2*$^{+/+}$

Rnd2, a member of the atypical Rho GTPase family, is involved in many pathways in this region (Fig. 3F). Our result also shows that the up-regulation of *Rnd2* mainly occurs in the IZ and part of CP (Fig. 3F) though other cell sources may have some contributions. It is reported that the ectopic expression of *Rnd2* disturbs the radial migration and then the cortical neuron development [29]. These results indicate that the *Satb2* possibly regulates the neuron growth and migration via the *Rnd2* in the IZ.

In the CP, the DEGs are highly enriched with the pathways involved in neuron morphology, migration and differentiation, such as synapse organization, axonogenesis, neuron migration, cytoskeleton organization, neuron differentiation, and etc. (Fig. 3E). For example, the lineage-specific gene *Tbr1* is down-regulated, and *Bcl11b* is up-regulated, consistent with the previous work that there exists complicated genetic network between *Satb2* and these genes in developing neocortex [30, 31]. In addition, the neuronal microtubule associated genes involved in cytoskeleton organization, such as *Tubb2b*, *Tubb3* and *Tubb5*, are largely down-regulated in the *Satb2*$^{-/-}$ mouse (Fig. 3F). Previous work showed that the CP can be further separated into the upper, middle and lower sub-layers [9], and then we tried to further cluster the CP using spatial transcriptomics data. These three sub-layers can be largely obtained in the *Satb2*$^{+/+}$ data, but the clustering is relatively messy in the *Satb2*$^{-/-}$ data (Supplementary Fig. 5), further indicating the ectopic gene expressions in the CP caused by *Satb2* ablation. For example, the neuropeptides related gene *Npy* is highly expressed in the CP in the *Satb2*$^{+/+}$ mouse, but its expression is significantly decreased in the *Satb2*$^{-/-}$ mouse (Fig. 3F, Supplementary Fig. 5). As for the pathway, we observed the enriched pathway of GTPase activity in the CP. Furthermore, the pathway of small GTPase mediated signal transduction is enriched in the IZ and CP (Fig. 3E). Considering the fact that the GTPase family, including the atypical Rnd member *Rnd2*, plays important roles in regulating the neuronal microtubule remodeling [32, 33], the aforementioned results imply that the dysregulated genes in GTPase family might lead to defect in microtubule associated genes or neuronal cytoskeleton, thus resulting in the defect in neuron morphology, migration and differentiation.

Validation on the key genes and relevant pathways

Finally, we performed cross-validations on the key downstream genes and relevant pathways regulated by *Satb2* using immunofluorescence or qPCR in population level (Fig. 4). Since it is reported that Pax6 and Tbr2 are sequentially expressed by radial glia and intermediate progenitor cells in neurogenesis [34], we first investigated these two factors. The Pax6^{+} cell number decreases to some extent (Fig. 4A), whereas the Tbr2^{+} cell number significantly increases in the VZ/SVZ and IZ in the *Satb2*$^{-/-}$ mice (Fig. 4B), suggesting that there exists abnormal differentiation from radial glia to intermediate progenitor cells. We further investigated the expression of Ki67, a proliferation marker involved in the regulation of mitotic nuclear division, and observed that the number of Ki67^{+} cells significantly increases in the VZ/SVZ and IZ (Fig. 4C), consistent with the cell number increase in the phenotype analysis (Fig. 2C). Considering the slight cell number decrease in the IZ derived from DAPI staining (Fig. 2C), this cell proliferation may imply that the cell types are decreased in the IZ. In the CP, the Tbr1^{+} cell number shows significant decrease (Fig. 4D), and the Bcl11b^{+} cell number shows significant increase in the *Satb2*$^{-/-}$ mice (Fig. 4E), consistent with the gene expression changes in spatial transcriptomics. Furthermore, the spatial relationship between Tbr1 and Bcl11b is also aberrantly changed in the *Satb2*$^{-/-}$ mice (Fig. 4F), suggesting the disrupted organization of these two lineage-specific markers. These immuno-staining results are also consistent with previous works [9, 10].

Since we did not find the proper antibodies for many key proteins, we used qPCR to validate the gene expressions in neocortex in population level. As shown in Fig. 4G, we validated the up-regulation of *Ldha* and *Rnd2*, and the down-regulation of *Sox11* and *Npy* in the *Satb2*$^{-/-}$ mice. Altogether, the immuno-staining and qPCR validate the key genes and relevant pathways derived from spatial transcriptomics, further suggesting that the neural precursor cells in VZ/SVZ and IZ undergo abnormally higher proliferation and differentiation, while the neuronal migration and specification are abnormal in the CP, partially due to the ectopic expressions of progenitor related factors and the members of GTPase family.

Discussion

Due to the importance of Satb2 in neocortical development, it is necessary to investigate its expression dynamics and regulatory pathways. Previous works have found the abnormal neocortical development in the *Satb2*-deficient mice, and they mainly focused on the role of Satb2 in regulating neuron specification and projection neuron development in the CP [9–12]. In this work, we utilized the spatial trancriptomics and immuno-staining to comprehensively investigate the region-specific genes and pathways regulated by Satb2, including the VZ/SVZ, IZ and CP. Our work finds that the *Satb2* loss leads to the thinner neocortex, consistent with previous works [9, 10]. By utilizing the spatial transcriptomics data, our work reveals that the lineage-specific genes, *Tbr1* and *Bcl11b*, are abnormally expressed in the CP in the *Satb2*-deficient mice. These regulatory relationships are consistent with previous works [30, 31], and confirm the roles of Satb2 in regulating upper-layer neuron specification and migration [9, 10]. However, our work further reveals

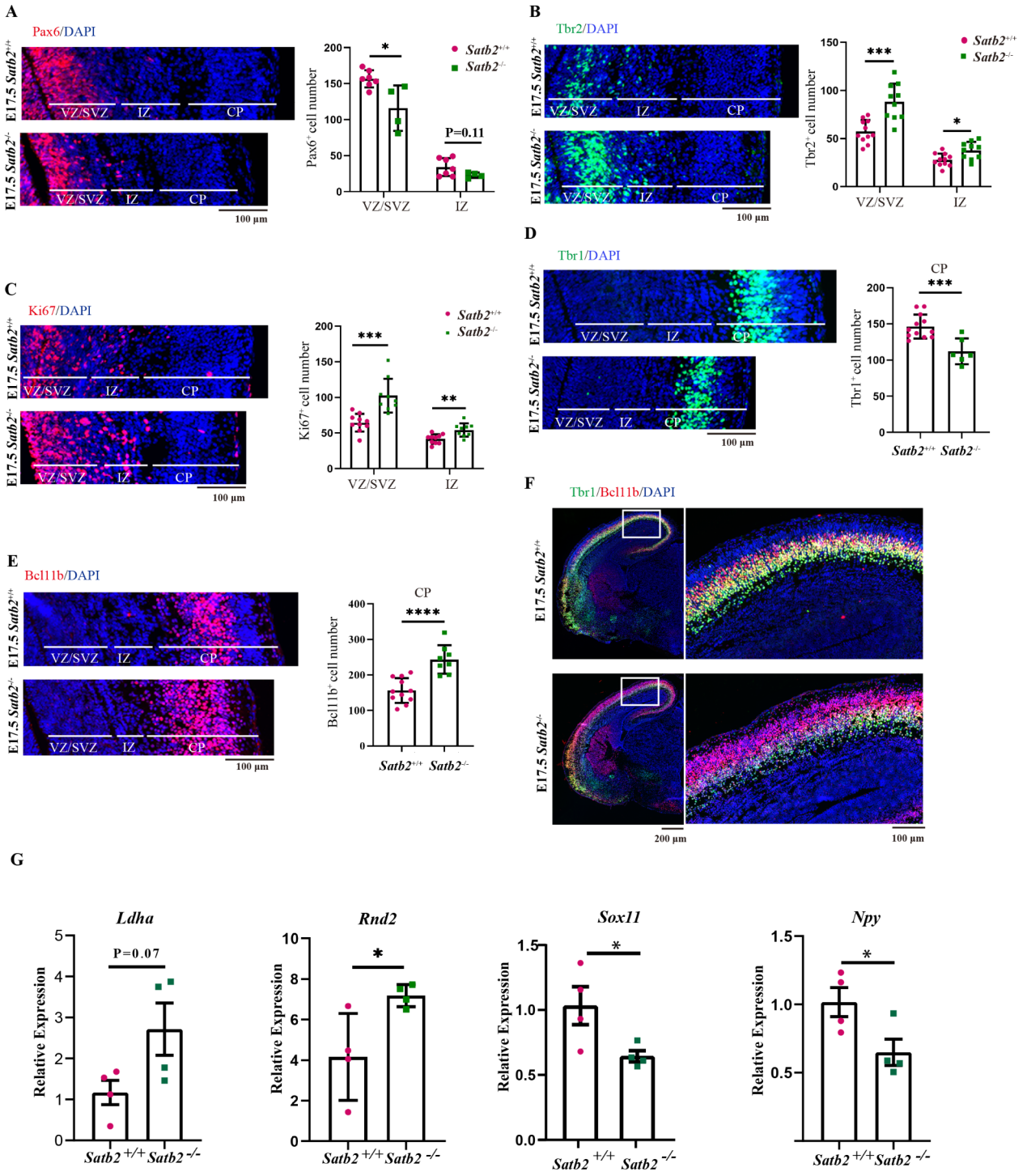

Fig. 4 Validation on the key factors. (**A**) Pax6. Sample size: *Satb2*$^{+/+}$, 7; *Satb2*$^{-/-}$, 4. (**B**) Tbr2. Sample size: *Satb2*$^{+/+}$, 11; *Satb2*$^{-/-}$, 10. (**C**) Ki67. Sample size: *Satb2*$^{+/+}$, 10; *Satb2*$^{-/-}$, 9. (**D**) Tbr1. Sample size: *Satb2*$^{+/+}$, 12; *Satb2*$^{-/-}$, 6. (**E**) Bcl11b. Sample size: *Satb2*$^{+/+}$, 11; *Satb2*$^{-/-}$, 8. (**F**) Co-staining of Tbr1 and Bcl11b. (**G**) The qPCR validations on genes *Lhda*, *Rnd2*, *Sox11* and *Npy*. The qPCR experiments were performed by using the whole neocortex. Sample size: *Satb2*$^{+/+}$, 4; *Satb2*$^{-/-}$, 4. In (**A**) to (**E**), the left one is the immuno-staining example, and the right one is the statistics in population level. The same or similar regions to Fig. 2 are selected in presentation and statistics

the potentially new genes regulated by Satb2, such as *Npy* [35], implying the ectopic neuropeptides in the neocortex in *Satb2*$^{-/-}$ mice.

Except the CP, we also utilized the spatial transcriptomics data and immuno-staining to explore the genes and pathways regulated by Satb2 in the VZ/SVZ and IZ, which were seldom studied in previous works. Our work reveals that there exist abnormal neural precursor cell proliferation and differentiation in the VZ/SVZ, and abnormal neuron growth and migration in the IZ. The spatial transcriptomics data also reveal the potentially key genes or gene families responsible for the observed defects in the VZ/SVZ and IZ in neocortical development. In the VZ/SVZ, the neural progenitor factors Pax6 and Tbr2 are dysregulated in the *Satb2*$^{-/-}$ mice. The genes involved in lactate production, such as *Ldha*, are up-regulated due to *Satb2* ablation. In the IZ, the *Satb2* loss leads to ectopic expressions for key genes in regulating neuronal differentiation and migration, such as *Sox11* and *Rnd2*. Though previous works reported that these genes can regulate the neural precursor cell proliferation, differentiation and migration in the VZ/SVZ or IZ [26–29, 36, 37], it is not yet clear that these genes can be regulated by *Satb2* in the neocortex. These findings are also interesting and intriguing since Satb2 is not co-expressed with neural precursor cell markers Pax6 and Tbr2 in the VZ/SVZ and IZ. However, the intermingled expressions between Satb2 and Pax6/Tbr2 are observed in the IZ during the early embryonic stages, implying that Satb2 could impact the neural progenitor cells in some indirect ways. It should be noted that we used the whole neocortical tissue for qPCR validation due to the difficulty in accurately dissecting the neocortical regions, and further works are needed to investigate the detailed mechanisms on how Satb2 regulates neural progenitor cells.

Conclusions

In summary, we explored the spatiotemporal expression dynamics between Satb2 and other layer markers during the embryonic development, revealing the complicated combinatorial expression patterns during embryonic development in this work. Our work also provides comprehensive exploration of the region-specific genes and pathways regulated by *Satb2* in neocortical development, which helps the understanding on this important neurodevelopmental disorder associated gene. However, due to the experimental variations in spatial transcriptomics and limited validations in this work, more thorough validations and works are still needed when further investigating the exact regulatory pathways in the future.

Abbreviations

SATB2 Special AT-rich binding protein 2
VZ Ventricle zone
SVZ Subventricle zone
IZ Intermediate zone
CP Cortical plate
DEG Differentially expressed gene

Supplementary Information

The online version contains supplementary material available at https://doi.org/10.1186/s12864-024-10672-w.

Supplementary Material 1

Supplementary Material 2

Supplementary Material 3

Acknowledgements

We thank Yuzhuo Zhou and Zongbo Zhang for helping the Stereo-seq experiment.

Author contributions

J.Y conducted the mouse husbandry and performed the experiments, and Y.L performed the data analysis. Y.T and J.Y performed the Stereo-seq experiments. L.Y participated in qPCR experiments. C.P and C.G conceived this project. C.P. administrated the project and wrote the manuscript. All authors read the manuscript.

Funding

This work was supported by the National Natural Science Foundation of China (32170662 to C.P., and 32070818 to C.G.), and Yunnan Fundamental Research Project (202401AS070131 to C.P., and 202001BB050005 to C.G.).

Data availability

The raw sequencing reads, coordinate file and image generated from Stereo-seq are deposited in National Genomics Data Center (https://ngdc.cncb.ac.cn) with the BioProject accession number PRJCA024751, in which the sequencing reads are under GSA accession number CRA015624, the coordinate file and image are under OMIX accession number OMIX006111.
The data analysis code is available at Github (https://github.com/liyu-ynu/Satb2/blob/main/Satb2.R).

Declarations

Ethics approval and consent to participate

This study has been approved by the Institutional Animal Care and Use Committee at Yunnan University with the approval number YNU20220244, and the animal experiments were conducted in compliance with the guideline.

Consent for publication

Not applicable.

Competing interests

The authors declare no competing interests.

Received: 15 April 2024 / Accepted: 29 July 2024
Published online: 02 August 2024

References

1. Holguera I, Desplan C. Neuronal specification in space and time. Science. 2018;362(6411):176–80.
2. Dobreva G, Dambacher J, Grosschedl R. SUMO modification of a novel MAR-binding protein, SATB2, modulates immunoglobulin μ gene expression. Genes Dev. 2003;17(24):3048–61.
3. Coe BP, Stessman HAF, Sulovari A, Geisheker MR, Bakken TE, Lake AM, Dougherty JD, Lein ES, Hormozdiari F, Bernier RA, et al. Neurodevelopmental disease genes implicated by de novo mutation and copy number variation morbidity. Nat Genet. 2019;51(1):106–16.

4. Mcrae JF, Clayton S, Fitzgerald TW, Kaplanis J, Prigmore E, Rajan D, Sifrim A, Aitken S, Akawi N, Alvi M, et al. Prevalence and architecture of de novo mutations in developmental disorders. Nature. 2017;542(7642):433–8.
5. Hong Y, Song K, Zhang Z, Deng Y, Zhang X, Zhao J, Jiang J, Zhang Q, Guo C, Peng C. The spatiotemporal dynamics of spatially variable genes in developing mouse brain revealed by a novel computational scheme. Cell Death Discovery 2023, 9(1).
6. Mukhtar T, Taylor V. Untangling cortical complexity during development. J Experimental Neurosci. 2018;12:1179069518759332–1179069518759332.
7. Britanova O, Akopov S, Lukyanov S, Gruss P, Tarabykin V. Novel transcription factor interacts with matrix attachment region DNA elements in a tissue-specific manner and demonstrates cell-type-dependent expression in the developing mouse CNS. Eur J Neurosci. 2005;21(3):658–68.
8. Dobreva G, Chahrour M, Dautzenberg M, Chirivella L, Kanzler B, Farinas I, Karsenty G, Grosschedl R. SATB2 is a multifunctional determinant of craniofacial patterning and osteoblast differentiation. Cell. 2006;125(5):971–86.
9. Alcamo EA, Chirivella L, Dautzenberg M, Dobreva G, Fariñas I, Grosschedl R, McConnell SK. Satb2 regulates callosal projection neuron identity in the developing cerebral cortex. Neuron. 2008;57(3):364–77.
10. Britanova O, de Juan Romero C, Cheung A, Kwan KY, Schwark M, Gyorgy A, Vogel T, Akopov S, Mitkovski M, Agoston D, et al. Satb2 is a postmitotic determinant for upper-layer neuron specification in the neocortex. Neuron. 2008;57(3):378–92.
11. Leone DP, Heavner WE, Ferenczi EA, Dobreva G, Huguenard JR, Grosschedl R, McConnell SK. Satb2 regulates the differentiation of both callosal and subcerebral projection neurons in the developing cerebral cortex. Cereb Cortex. 2015;25(10):3406–19.
12. Zhang L, Song N-N, Chen J-Y, Huang Y, Li H, Ding Y-Q. Satb2 is required for dendritic arborization and Soma Spacing in Mouse Cerebral cortex. Cereb Cortex. 2012;22(7):1510–9.
13. Zhang L, Song NN, Zhang Q, Mei WY, He CH, Ma PC, Huang Y, Chen JY, Mao BY, Lang B, et al. Satb2 is required for the regionalization of retrosplenial cortex. Cell Death Differ. 2020;27(5):1604–17.
14. Zhang Q, Zhang L, Huang Y, Ma PC, Mao BY, Ding YQ, Song NN. Satb2 regulates the development of dopaminergic neurons in the arcuate nucleus by Dlx1. Cell Death Dis 2021, 12(10).
15. Zarate YA, Fish JL. *SATB2*-associated syndrome: mechanisms, phenotype, and practical recommendations. Am J Med Genet A. 2017;173(2):327–37.
16. Cheng M, Jiang Y, Xu J, Mentis A-FA, Wang S, Zheng H, Sahu SK, Liu L, Xu X. Spatially resolved transcriptomics: a comprehensive review of their technological advances, applications, and challenges. J Genet Genomics. 2023;50(9):625–40.
17. Ortiz C, Navarro JF, Jurek A, Märtin A, Lundeberg J, Meletis K. Molecular atlas of the adult mouse brain. *Sci Adv* 2020, 6(26).
18. Di Bella DJ, Habibi E, Stickels RR, Scalia G, Brown J, Yadollahpour P, Yang SM, Abbate C, Biancalani T, Macosko EZ, et al. Molecular logic of cellular diversification in the mouse cerebral cortex. Nature. 2021;595(7868):554–9.
19. Chen A, Sun Y, Lei Y, Li C, Liao S, Meng J, Bai Y, Liu Z, Liang Z, Zhu Z, et al. Single-cell spatial transcriptome reveals cell-type organization in the macaque cortex. Cell. 2023;186(17):3726–e37433724.
20. Li Y, Li Z, Wang C, Yang M, He Z, Wang F, Zhang Y, Li R, Gong Y, Wang B, et al. Spatiotemporal transcriptome atlas reveals the regional specification of the developing human brain. Cell. 2023;186(26):5892–e59095822.
21. Dobin A, Davis CA, Schlesinger F, Drenkow J, Zaleski C, Jha S, Batut P, Chaisson M, Gingeras TR. STAR: ultrafast universal RNA-seq aligner. Bioinformatics. 2013;29(1):15–21.
22. Hao Y, Stuart T, Kowalski MH, Choudhary S, Hoffman P, Hartman A, Srivastava A, Molla G, Madad S, Fernandez-Granda C, et al. Dictionary learning for integrative, multimodal and scalable single-cell analysis. Nat Biotechnol. 2024;42(2):293–304.
23. Qiu XJ, Mao Q, Tang Y, Wang L, Chawla R, Pliner HA, Trapnell C. Reversed graph embedding resolves complex single-cell trajectories. Nat Methods. 2017;14(10):979–82.
24. Wu TZ, Hu EQ, Xu SB, Chen MJ, Guo PF, Dai ZH, Feng TZ, Zhou L, Tang WL, Zhan L et al. clusterProfiler 4.0: a universal enrichment tool for interpreting omics data. Innovation-Amsterdam 2021, 2(3).
25. Chen A, Liao S, Cheng MN, Ma KL, Wu L, Lai YW, Qiu XJ, Yang J, Xu JS, Hao SJ, et al. Spatiotemporal transcriptomic atlas of mouse organogenesis using DNA nanoball-patterned arrays. Cell. 2022;185(10):1777–92.
26. Scott CE, Wynn SL, Sesay A, Cruz C, Cheung M, Gaviro MVG, Booth S, Gao B, Cheah KSE, Lovell-Badge R, et al. SOX9 induces and maintains neural stem cells. Nat Neurosci. 2010;13(10):1181–9.
27. Dong XX, Zhang QQ, Yu XY, Wang D, Ma JM, Ma J, Shi SH. Metabolic lactate production coordinates vasculature development and progenitor behavior in the developing mouse neocortex. Nat Neurosci. 2022;25(7):865–75.
28. Li YZ, Wang JJ, Zheng YR, Zhao Y, Guo M, Li Y, Bao QL, Zhang Y, Yang LZ, Li QS. Sox11 modulates neocortical development by regulating the proliferation and neuronal differentiation of cortical intermediate precursors. Acta Bioch Bioph Sin. 2012;44(8):660–8.
29. Nakamura K, Yamashita Y, Tamamaki N, Katoh H, Kaneko T, Negishi M. In vivo function of Rnd2 in the development of neocortical pyramidal neurons. Neurosci Res. 2006;54(2):149–53.
30. Srinivasan K, Leone DP, Bateson RK, Dobreva G, Kohwi Y, Kohwi-Shigematsu T, Grosschedl R, McConnell SK. A network of genetic repression and derepression specifies projection fates in the developing neocortex. P Natl Acad Sci USA. 2012;109(47):19071–8.
31. McKenna WL, Ortiz-Londono CF, Mathew TK, Hoang K, Katzman S, Chen B. Mutual regulation between and Satb2 and Fezf2 promotes subcerebral projection neuron identity in the developing cerebral cortex. P Natl Acad Sci USA. 2015;112(37):11702–7.
32. Ayala R, Shu TZ, Tsai LH. Trekking across the brain: the journey of neuronal migration. Cell. 2007;128(1):29–43.
33. Cooper JA. Mechanisms of cell migration in the nervous system. J Cell Biol. 2013;202(5):725–34.
34. Englund C, Fink A, Lau C, Pham D, Daza RAM, Bulfone A, Kowalczyk T, Hevner RF. Pax6, Tbr2, and Tbr1 are expressed sequentially by radial glia, intermediate progenitor cells, and postmitotic neurons in developing neocortex. J Neurosci. 2005;25(1):247–51.
35. Bale R, Doshi G. Cross talk about the role of Neuropeptide Y in CNS disorders and diseases. Neuropeptides 2023, 102.
36. Yun K, Mantani A, Garel S, Rubenstein J, Israel MA. Id4 regulates neural progenitor proliferation and differentiation in vivo. Development. 2004;131(21):5441–8.
37. Wang JB, Wang AD, Tian K, Hua XJ, Zhang B, Zheng Y, Kong XF, Li W, Xu LC, Wang J et al. A *Ctnnb1* enhancer regulates neocortical neurogenesis by controlling the abundance of intermediate progenitors. Cell Discov 2022, 8(1).

Publisher's Note